Thermal management of the remote phosphor layer in LED systems

Indika U. Perera and Nadarajah Narendran*
Lighting Research Center, Rensselaer Polytechnic Institute, 21 Union St., Troy, NY 12180 USA

ABSTRACT

Generally in a white light-emitting diode (LED), a phosphor slurry is placed around the semiconductor chip or the phosphor is conformally coated over the chip to covert the narrowband, short-wavelength radiation to a broadband white light. Over the past few years, the remote-phosphor method has provided significant improvement in overall system efficiency by reducing the photons absorbed by the LED chip and reducing the phosphor quenching effects. However, increased light output and smaller light engine requirements are causing high radiant energy density on the remote-phosphor plates, thus heating the phosphor layer. The phosphor layer temperature rise increases when the phosphor material conversion efficiency decreases. Phosphor layer heating can negatively affect performance in terms of luminous efficacy, color shift, and life. In such cases, the performance of remote-phosphor LED lighting systems can be improved by suitable thermal management to reduce the temperature of the phosphor layer. To verify this hypothesis and to understand the factors that influence the reduction in temperature, a phosphor layer was embedded in a perforated metal heatsink to remove the heat; the parameters that influence the effectiveness of heat extraction were then studied. These parameters included the heatsink-to-phosphor layer interface area and the thermal conductivity of the heatsink. The temperature of the remote-phosphor surface was measured using IR thermography. The results showed that when the heat conduction area of the heatsink increased, the phosphor layer temperature decreased, but at the same time the overall light output of the remote phosphor light engine used in this study decreased due to light absorption by the metal areas.

Keywords: light-emitting diode, remote phosphor, thermal management, solid-state lighting, down-conversion, IR thermography, extended-surface heat conduction

1. INTRODUCTION

There are two main components in a phosphor-converted white LED package that convert energy: 1) the LED chip that converts electrical energy to a short-wavelength visible radiant energy, and 2) the phosphor material that down-converts the short-wavelength visible radiation to a broadband long-wavelength visible radiation [1],[2] The heat generation inside a phosphor-converted white LED package is mostly due to the inefficiencies in these conversion processes.

At present, the heat generation within an LED and the effect of this heat on LED performance is well understood [3]. With the industry moving toward higher lumen packages with smaller footprint light engines, there is significant research interest in understanding the heat production within the phosphor layer and its effects. Generally, phosphor conversion efficiency is negatively affected by an increase in temperature [4]. In addition, the temperature rise affects the binding material used in creating the phosphor layers and reduces the overall light output of the LED. The temperature rise caused by a reduced phosphor conversion efficiency and additional light absorption by the binding material accelerates lumen degradation and reduces system useful lifetime [5].

In a white LED system, the amount of phosphor layer heat buildup depends on a number factors that include: 1) the location of the phosphor, 2) the thickness and concentration of the phosphor layer, 3) the binding media used in creating the phosphor layer, 4) the LED chip and package structure, and 5) the phosphor conversion efficiency [1],[2],[6]-[8].

Past studies have observed the heat generated in the phosphor layer, caused by the conversion efficiency losses (quantum conversion losses and Stokes shift losses) and trapped photons in the phosphor layer (due to total internal reflection and Fresnel reflection), can be as high as 13% of the total input electrical power to the LED system [8]. Furthermore, studies have stated this generated heat in the phosphor layer can increase the operational temperature of the phosphor layer to greater than 150°C [2],[7].

*Corresponding author: +1 (518) 687-7100; narenn2@rpi.edu; http://www.lrc.rpi.edu/programs/solidstate/

LED-based Illumination Systems, edited by Jianzhong Jiao, Proc. of SPIE Vol. 8835, 883504 · © 2013 SPIE · CCC code: 0277-786X/13/$18 · doi: 10.1117/12.2023094

As a solution to this heat buildup in phosphor layers, some studies have investigated thermally conductive binding media, such as glass and alumina, for fabricating the phosphor layer [1], while others have studied pulsed operation to reduce the phosphor operation temperature [2]. In addition to these studies, dedicated thermal management of the phosphor layer has been pursued with the use of a thermally conducting material attached to the phosphor layer [9].

The operating temperature of the phosphor layer becomes a critical parameter in determining the useful system lifetime, and therefore, investigation of a thermal management method that could reduce the operating temperature of the phosphor layer and analyzing the effect of the thermal management method on the overall optical performance of the LED system were the goals of this study.

2. METHODOLOGY

A metal heatsink, similar to those shown in Figure 1, was used to conduct the heat away from the phosphor layer to the surrounding ambient. It was hypothesized that by increasing the contact surface area between the phosphor layer and the heatsink, the temperature of the phosphor layer would decrease. Three heatsink configurations with varying heat conduction area (Table 1) were used to investigate the effect of increased heat conduction area on phosphor layer temperature. It was also hypothesized that heatsinks with higher thermal conductivity would reduce the temperature of the phosphor layer. Aluminum and acrylic heatsinks were used for investigating the thermal conductivity effect on phosphor layer temperature.

Table 1. Heatsink configurations

Thickness of all heatsinks = 1.5 mm						
	Diameter of the hole (mm)	**Number of holes**	**Emitting surface area (mm^2)**	**Emitting surface area ratio**	**Conduction area (mm^2)**	**Conduction area ratio**
Heatsink #1	19.1	1	285	1.0	90	1.0
Heatsink #2	7.2	7	286	1.0	238	2.6
Heatsink #3	4.4	19	285	1.0	391	4.4

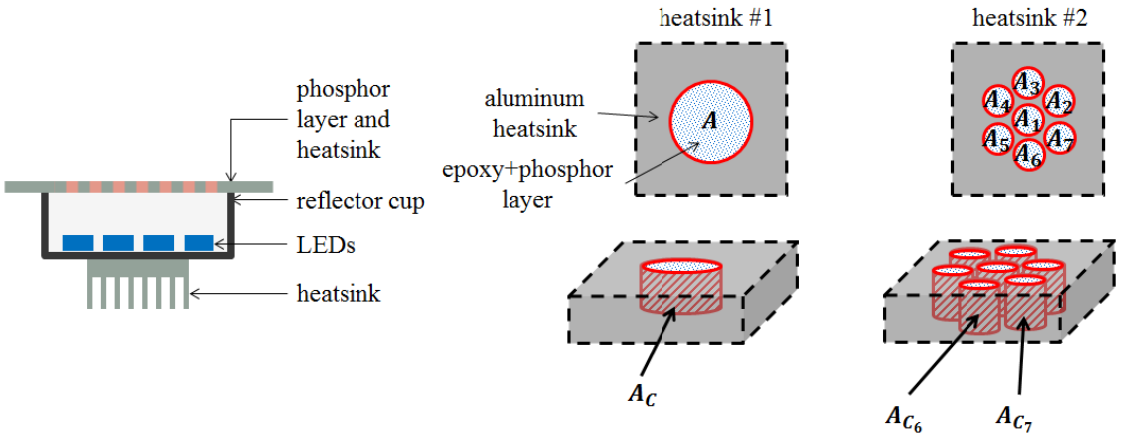

Figure 1. Sketch of LED light engine setup and heatsink (left), and sketch of heatsinks #1 and #2 with embedded phosphor and epoxy layer (right)

A sketch of the LED light engine assembly for irradiating the phosphor layer embedded in the heatsink is illustrated in Figure 1 (left). The short-wavelength irradiance on the phosphor layer was maintained at a constant value by controlling the drive current of the LEDs and maintaining the same estimated junction temperature of the LEDs. The distance from the LEDs to the phosphor layer-embedded heatsink was also maintained at a constant distance. The three phosphor-embedded heatsink configurations had equal emitting surface areas, as indicated in Table 1 and as illustrated in Figure 1 (right). The emitting surface area A of heatsink #1 and the total emitting surface area, which is the summation of surface areas A_1 through A_7 in heatsink #2, are equal. Similarly, heatsink #3 had the same emitting surface area as the other heatsinks (Table 1). The reason for keeping the emitting areas the same was to ensure the same visible radiant power. On

the other hand, the heat conduction area, which is the interfacial surface area between the phosphor layer and the heatsink material, increases as the number of holes increase (Table 1). As an example, the conduction area in heatsink #1, A_C, is smaller than the total area in heatsink #2 in Figure 1 (right). This increase in the heat conduction area would increase the amount of heat transferred from the phosphor layer to the heatsink, given that the heatsink is effective in dissipating the heat to the ambient.

3. EXPERIMENT

A number of LEDs (peak wavelength ~448 nm) were arranged on an LED heatsink and reflector cup assembly to generate a uniform irradiance on the phosphor plate at a fixed distance from the LEDs. The LED operation temperature was maintained at a fixed temperature at the reference location specified by the LED manufacturer with the use of a cooling fan and a heating element controlled by a temperature control system, as illustrated in Figure 2.

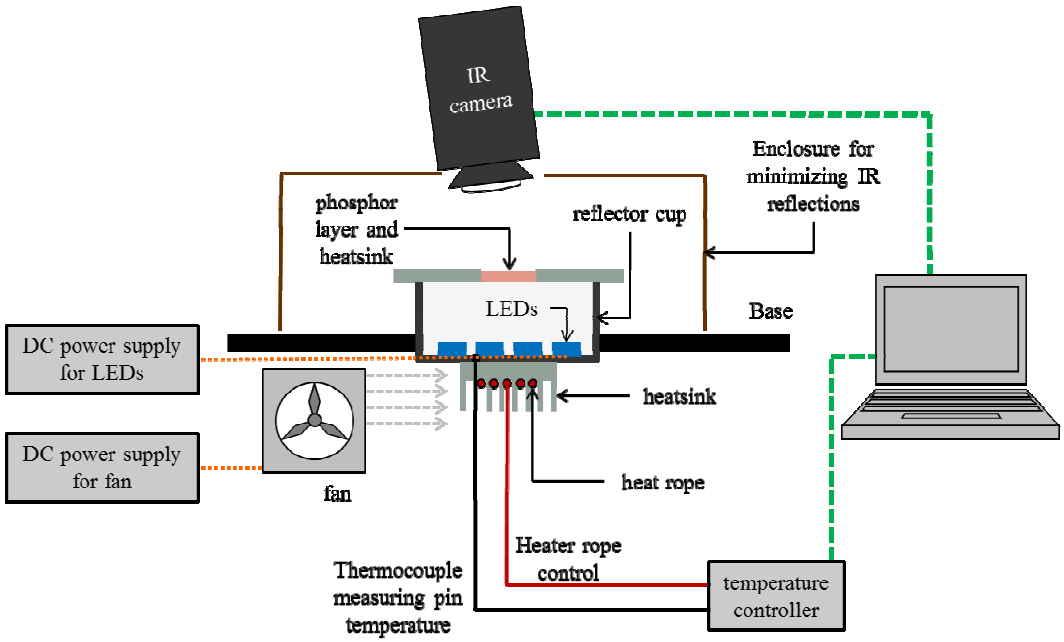

Figure 2. Experimental setup for surface temperature measurement including the IR imaging camera

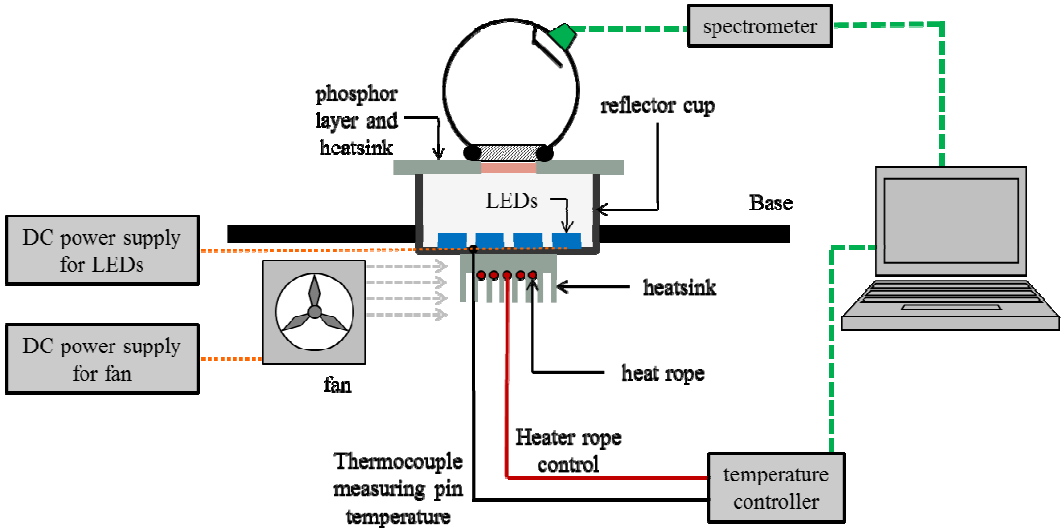

Figure 3. Experimental setup for visible radiant power with sphere-spectrometer system

The machined aluminum and acrylic heatsinks were embedded with the same phosphor-to-epoxy concentration mixture (1:10 ratio by weight). The aluminum and acrylic heatsink surfaces facing the LEDs were painted white to achieve similar surface properties. Surface temperature of the phosphor layer and heatsink, and visible radiant power emitted from the phosphor layer and heatsink were alternatively measured with the equipment illustrated in Figure 2 and Figure 3, respectively.

An IR camera (spectral sensitivity: 7.5–14 μm) was used to measure the surface temperature of the phosphor layer-embedded heatsink with an estimated target surface emissivity. The surface temperature was measured at the geometric center of the phosphor layer-embedded heatsink assembly, as illustrated in Figure 4. All temperature measurements were conducted at steady-state operation of the LEDs and steady-steady temperature of the phosphor layer-embedded heatsink. A sphere-spectrometer system was used to measure the visible radiant power. The steady-state visible radiant power was measured at steady-state operation of the LEDs and the phosphor layer-embedded heatsink.

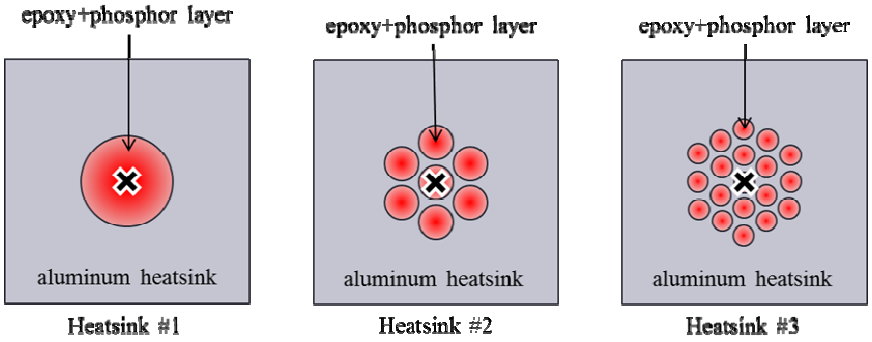

Figure 4. Geometric center temperature measurement location on heatsink configurations

4. RESULTS

Due to the physical symmetry of the heatsink configurations, the steady-state temperature at the geometric center location of the phosphor layer-embedded heatsink was used for analysis of heatsink effectiveness. Table 2 shows the results for the aluminum heatsink configurations for the geometric center temperature and the visible radiant power of each heatsink configuration relative to heatsink #1. Increasing the conduction area from heatsink #1 to heatsink #2 reduced the geometric center temperature by 25%, but the relative visible radiant power also reduced by 11%. The increase in heat conduction area by 2.6 times reduced the phosphor operation maximum temperature considerably at a loss of one-tenth of the optical power. Further increasing the heat conduction area of heatsink #3 to 4.4 times that of heatsink #1 reduced the maximum temperature by 29% while the relative radiant power reduced by 33%. The further increase did not provide much benefit with respect to thermal management while the optical performance drastically reduced when the heat conduction area ratio was increased greater than 2.6 times the heat conduction area of heatsink #1.

Table 2. Geometric center temperature and relative visible radiant power results for aluminum heatsink configurations

	Heatsink #1		Heatsink #2		Heatsink #3	
	Avg.	**Std. Dev.**	**Avg.**	**Std. Dev.**	**Avg.**	**Std. Dev.**
Geometric center temperature (°C)	110.8	1.5	83.5 (-25%)	0.2	79.1 (-29%)	1.2
Relative visible radiant power	100%	0%	89% (-11%)	2%	67% (-33%)	1%

The results in Table 2 support the hypothesis that an increased heat conduction area of the heatsink leads to lower operation temperature of the phosphor layer. However, at the same time, the overall light output of the remote phosphor light engine used in this study decreased.

Table 3. Geometric center temperature measurements from aluminum and acrylic heatsinks

Heatsink material	Geometric center temperature (°C)					
	Heatsink #1		Heatsink #2		Heatsink #3	
	Avg.	Std. Dev.	Avg.	Std. Dev.	Avg.	Std. Dev.
Aluminum	110.8	1.5	83.5	0.2	79.1	1.2
Acrylic	125.8	2.1	126.3	0.2	127.3	0.3

Table 3 shows the effect of thermal conductivity of the heatsink material on reducing phosphor layer temperature. The aluminum heatsink reduced the geometric center temperature as the heat conduction area was increased while no reduction in the geometric center temperature was observed with acrylic heatsinks when the heat conduction area was increased. In addition, the acrylic heatsinks displayed higher phosphor operational temperature for all tested heatsink conduction area configurations. These results illustrate that the geometrical aspects of the heatsink and thermal properties of the heatsink material are important in this thermal management method.

LightTools®, a commercial ray-tracing simulation software, was used to systematically analyze the reduction of visible radiant power when the heat conduction area was increased. The phosphor layer was modeled as a non-scattering medium with a constant refractive index for these numerical simulations while the internal surface reflectivities were changed systematically. These surfaces were considered as optical absorbers when the surface reflectivities were not equal to unity. Figure 5 shows the different internal surfaces of the LED light engine setup where the surface reflectance was varied.

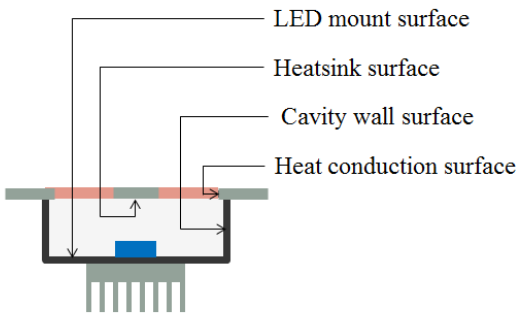

Figure 5. Sketch of LED light engine setup internal surfaces

Reduction in surface reflectivity decreased the visible radiant power output from the LED light engine due to the surface absorption of photons. The visible radiant power output reduction was higher for the LED mount surface, the heatsink underside surface, and the cavity wall (reflector cup) surface reflectivity reduction. The visible radiant power output reduction was lower for the heatsink conduction surface reflectivity reduction compared to the other surfaces stated above.

The visible radiant power output change was small (<5%) among the heatsink configurations for all internal LED light engine surfaces except for the heatsink conduction surface. The change in heatsink configurations was ~10-15% with respect to visible radiant output power for the heatsink conduction surface as the heatsink conduction area surface reflectivity was reduced.

These findings provide a plausible explanation for the reduced visible radiant power when the heat conduction area was increased. The increased conduction area improved heat transfer but it also increased the surface absorption of photons, thus reducing the visible radiant power. A similar trend was observed with the reflectivity of the cavity surface and the LED mount surface.

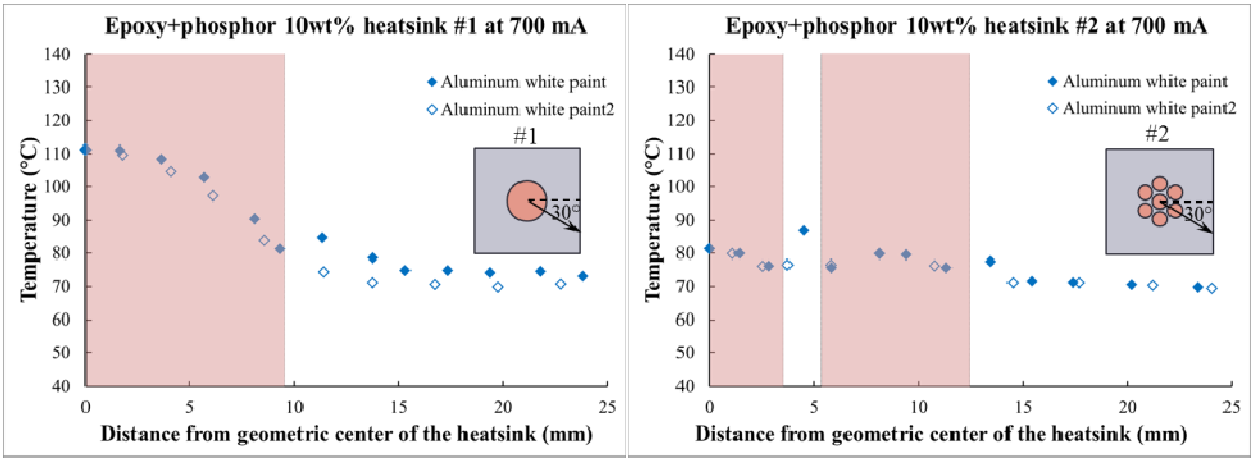

Figure 6. Surface temperature profile of heatsinks #1 and #2

Figure 6 shows the surface temperature profile along a radial direction of the phosphor layer and heatsink. The radial direction is illustrated in the inset diagrams. Heatsink #2 not only had a lower maximum phosphor layer operating temperature compared to heatsink #1, it also maintained a lower uniform operating temperature across the entire phosphor layer. The surface temperature profile of heatsink #3 was similar to heatsink #2. The lower phosphor layer temperature reduces the lumen depreciation due to binding material degradation and increases the conversion efficiency of the phosphor compared to phosphor and binding material operating at a higher temperature.

5. DISCUSSION

The use of metal heatsinks reduced heat buildup in the phosphor layer by effectively extracting the heat and efficiently transferring it to the ambient. The effectiveness of heat transfer of these metal heatsinks depends on the geometry and the thermal conduction properties. The heatsinks used in the present study reduced the phosphor layer temperature but also reduced the visible radiant power. As part of an ongoing study, the authors are investigating other heatsink and light engine configurations to improve overall light output while reducing the phosphor layer temperature.

ACKNOWLEDGMENTS

The authors would like to acknowledge the financial support of the Lighting Research Center at Rensselaer Polytechnic Institute, Henkel, and the Besal Lighting Education Fund provided by Acuity Brands Lighting; and the contribution and support of Russell Leslie, Andrew Bierman, Jean Paul Freyssinier, Yi-wei Liu, Martin Overington, and Jennifer Taylor at the Lighting Research Center.

REFERENCES

[1] Wiesmann, Ch., Linkov, A., and Muschaweck, J., “Estimating the performance of remote phosphor SSL devices by simulations,” Proc. SPIE 8550, 85502G-1-5 (2012). doi: 10.1117/12.2001607

[2] Wenzl, F. -P., Sommer, C., Hartmann, P., Pachler, P., Hoschopf, H., Langer, G., Fulmek, P., and Nicolics, J., “The impact of the non-linearity of the radiant flux on the thermal load of the color conversion elements in phosphor converted LEDs under different current driving schemes,” Opt. Express 21 (S3), A439-A449 (2013). doi: 10.1364/OE.21.00A439

[3] Arik, M., Becker, C., Weaver, S., and Petroski, J., “Thermal management of LEDs: Package to system,” Proc. SPIE 5187, 64-75 (2004). doi: 10.1117/12.512731

[4] Lin, C. -C., and Liu, R. -S., “Advances in phosphors for light-emitting diodes,” J. Phys. Chem. Lett. 2 (11), 1268-1277 (2011). doi: 10.1021/jz2002452

[5] Narendran, N., Maliyagoda, N., Bierman, A., Pysar, R., and Overington, M., “Characterizing white LEDs for general illumination applications,” Proc. SPIE 3938, 240-248 (2000). doi:10.1117/12.382836

[6] Hu, R., Luo, X., and Zheng, Z., "Hotspot location shift in the high-power phosphor-converted white light-emitting diode packages," Jpn. J. Apply. Phys. 51, 09MK05-1-4 (2012). doi: 10.1143/JJAP.51.09MK05
[7] Luo, X., Fu, X., Chen, F., and Zheng, H., "Phosphor self-heating in phosphor converted light emitting diode packaging," Int. J. Heat Mass Tran. 58 (1-2), 276-281 (2013). doi.org/10.1016/j.ijheatmasstransfer.2012.11.056
[8] Huang M., and Yang, L., "Heat generation by the phosphor layer of high-power white LED emitters," IEEE Photonics Technol. Lett. 25 (4), 1317-1320 (2013). doi: 10.1109/LPT.2013.2263375
[9] Lowery, C., "Methods and apparatuses for enhancing heat dissipation from a light emitting device," U.S. Patent 8 076 833 B2, Dec. 13, 2011.